EuroIntervention 2020;16:395-403 published online April 2020

Special feature: Plaque characteristics

Detection of cholesterol crystals by optical coherence tomography

Hiroyuki Jinnouchi[1], MD; Yu Sato[1], MD; Sho Torii[1], MD; Atsushi Sakamoto[1], MD; Anne Cornelissen[1], MD; Rahul R. Bhoite[1], MD; Salome Kuntz[1], MD; Liang Guo[1], PhD; Ka Hyun Paek[1], BS; Raquel Fernandez[1], BS; Frank D. Kolodgie[1], PhD; Renu Virmani[1], MD; Aloke V. Finn[1,2]*, MD

1. CVPath Institute, Gaithersburg, MD, USA; 2. University of Maryland, School of Medicine, Baltimore, MD, USA

This paper also includes supplementary data published online at: https://eurointervention.pcronline.com/doi/10.4244/EIJ-D-20-00202

KEYWORDS

- ACS/NSTE-ACS
- other imaging modalities
- stable angina

Abstract

Aims: The aim of this study was to determine the ability of optical frequency domain imaging (OFDI)/optical coherence tomography (OCT) imaging systems to visualise the presence of cholesterol crystals (CCR) in human atherosclerotic coronary arteries.

Methods and results: We performed *ex vivo* imaging of human coronary arteries by OFDI/OCT. A total of 559 cross-sectional images from 45 autopsy cases were co-registered with histology; 117 histologic sections showed presence of necrotic core with cholesterol clefts (CC). We modified a previously used OFDI/OCT definition for identification of CCRs which we now define as a linear and discrete high-intensity signal (bright area) within the plaque with sharp borders between it and adjacent low-/intermediate-intensity tissue. Additionally, the high-intensity signal is not a spot but a well-defined area distinguishing it from macrophages which lack sharp borders. OFDI/OCT imaging identified the presence of CCR in 30 of the 117 histologic sections. The sensitivity and specificity of OFDI/OCT for detection of CCR was 25.6% and 100.0%, respectively. By multivariate analysis, significant predictors to visualise CCR by OCT/OFDI were 1) an overlying fibrous plaque, and 2) the presence of stacked CC, defined as CC arranged one on top of another with >3 layers of CC. The prevalence of complicated plaques (i.e., plaque haemorrhage and late necrotic core) was significantly higher in detectable CCR by OFDI/OCT as compared to undetectable CCR.

Conclusions: The presence of stacked CCs is required to detect CCR by OFDI/OCT. Detection of CCR by OCT/OFDI may help us to identify the late stages of atherosclerotic coronary plaque progression and improve risk stratification.

**Corresponding author: CVPath Institute, Inc., 19 Firstfield Road, Gaithersburg, MD 20878, USA. E-mail: AFinn@CVPath.org*

SUBMITTED ON 18/02/2020 - REVISION RECEIVED ON 09/04/2020 - ACCEPTED ON 17/04/2020

DOI: 10.4244/EIJ-D-20-00202

Abbreviations

AIT	adaptive intimal thickening
CC	cholesterol cleft
CCR	cholesterol crystals
EEL	external elastic lamina
FA	fibroatheroma
IEL	internal elastic lamina
OCT	optical coherence tomography
OFDI	optical frequency domain imaging
PIT	pathological intimal thickening
TCFA	thin-cap fibroatheroma

Introduction

Atherosclerotic coronary artery disease is the leading cause of death worldwide. Many studies have reported on the mechanisms of progression of atherosclerotic lesions. Atherosclerotic plaques develop through the deposition of lipid in acellular areas of the intima which are rich in proteoglycans, and form what is known as a lipid pool. Lipid pools are mostly devoid of cholesterol crystals (CCR) but progress to form necrotic cores by macrophage infiltration and subsequent phagocytosis of lipid which causes them eventually to undergo apoptosis, forming acellular debris with the release of free cholesterol[1]. Free cholesterol has also been shown to be derived from red cell membranes that are observed as plaques thicken and vasa vasorum rupture leading to intraplaque haemorrhages. Plaque rupture is the most frequent cause of acute coronary syndromes[1]. Necrotic cores are composed of acellular debris rich in CCR which are formed by the crystallisation of free cholesterol. Recent studies have shown that CCR trigger inflammation by the release inflammasomes which facilitate the development of lipid-rich necrotic core[2]. The presence of CCR is associated with worse clinical outcomes through distal embolisation in patients receiving percutaneous coronary intervention[3]. Therefore, the presence of CCR has been considered to be an indicator of advanced plaque.

Diagnostic modalities that have the ability to identify plaque composition could be used to improve risk stratification and to guide therapy to prevent untoward cardiovascular events. Optical frequency domain imaging (OFDI) and optical coherence tomography (OCT) imaging are high-resolution intravascular imaging modalities that provide a maximal axial resolution of 10-20 µm, allowing identification of tissue characteristics. However, not all CCR are detectable by OFDI/OCT. The reason why CCR are detectable in some plaques and not in others remains unclear. In addition, the pathophysiological significance of the presence of detectable CCR is unknown. To the best of our knowledge, there are no studies examining the accuracy of OFDI/OCT for detection of CCR. Our study sought to evaluate whether CCR could be identified by OFDI/OCT (with histology as the gold standard) and to determine why some CCR are detectable by OFDI/OCT while others remain undetectable in human coronary arteries.

Editorial, see page 364

Methods

STUDY POPULATION

A total of 55 vessels from 45 patients underwent OFDI or OCT with corresponding histologic sections and were included in the study. **Supplementary Appendix 1** provides more details.

CO-REGISTRATION OF OFDI/OCT IMAGES WITH HISTOLOGY

All OFDI and OCT images were co-registered with histologic sections by an experienced investigator (H. Jinnouchi). For careful co-registration between OFDI/OCT images and histological sections, side branches and the distance from the nearest ostium were taken into consideration, and anatomical landmarks such as calcification and luminal configuration were considered to adjust images longitudinally and circumferentially.

CLASSIFICATION OF ATHEROSCLEROTIC PLAQUES IN HISTOLOGY

All histology slides were reviewed by experienced readers (H. Jinnouchi and R. Virmani). Coronary plaques were classified using the modified American Heart Association classification: 1) adaptive intimal thickening (AIT) or fibrous plaque (FIB), defined as lesions with predominantly fibrous tissue and no lipid pool; 2) pathological intimal thickening (PIT), defined as lesions with lipid pools but absence of necrosis; 3) fibroatheroma (FA), defined as plaques containing necrotic core (±plaque haemorrhage) with thick fibrous cap thickness (>65 µm); 4) thin-cap fibroatheroma (TCFA), defined as FA with the thinnest portion of the fibrous cap ≤65 µm in thickness and the cap infiltrated by macrophages and lymphocytes with an underlying necrotic core (±plaque haemorrhage); 5) fibrocalcific plaque, defined as lesions with severe calcification with absence or only a small fraction of necrotic core; and 6) plaque rupture with a disrupted fibrous cap and an overlying thrombus. FA was further divided into early and late FA dependent on the presence or absence of a matrix (proteoglycan or collagen)[1]. Early FA was defined as plaques with necrotic core in which focal free cholesterol may be present with focal loss of proteoglycans and/or collagen with macrophage infiltration, whereas late FA was defined as plaque with necrotic core and nearly complete depletion of the extracellular matrix with increase in free cholesterol clefts (CC). In addition, all plaques with necrotic cores were classified as early and late necrotic core, including FA, TCFA and plaque rupture. The overlying plaque (above the necrotic core) was also assessed for presence of fibrous tissue, presence or absence of high density of foamy macrophages, calcification, PIT lesion and overlying thrombus. Stacked CC were defined as multiple large CC overlying one another with greater than three layers of CC within areas of necrotic core **(Figure 1)**.

OFDI AND OCT IMAGING ANALYSIS

Two OFDI/OCT readers (Y. Sato and A. Sakamoto) blinded to the histologic findings assessed OFDI/OCT images independently. The prior definition of CCR as a "high linear signal within the

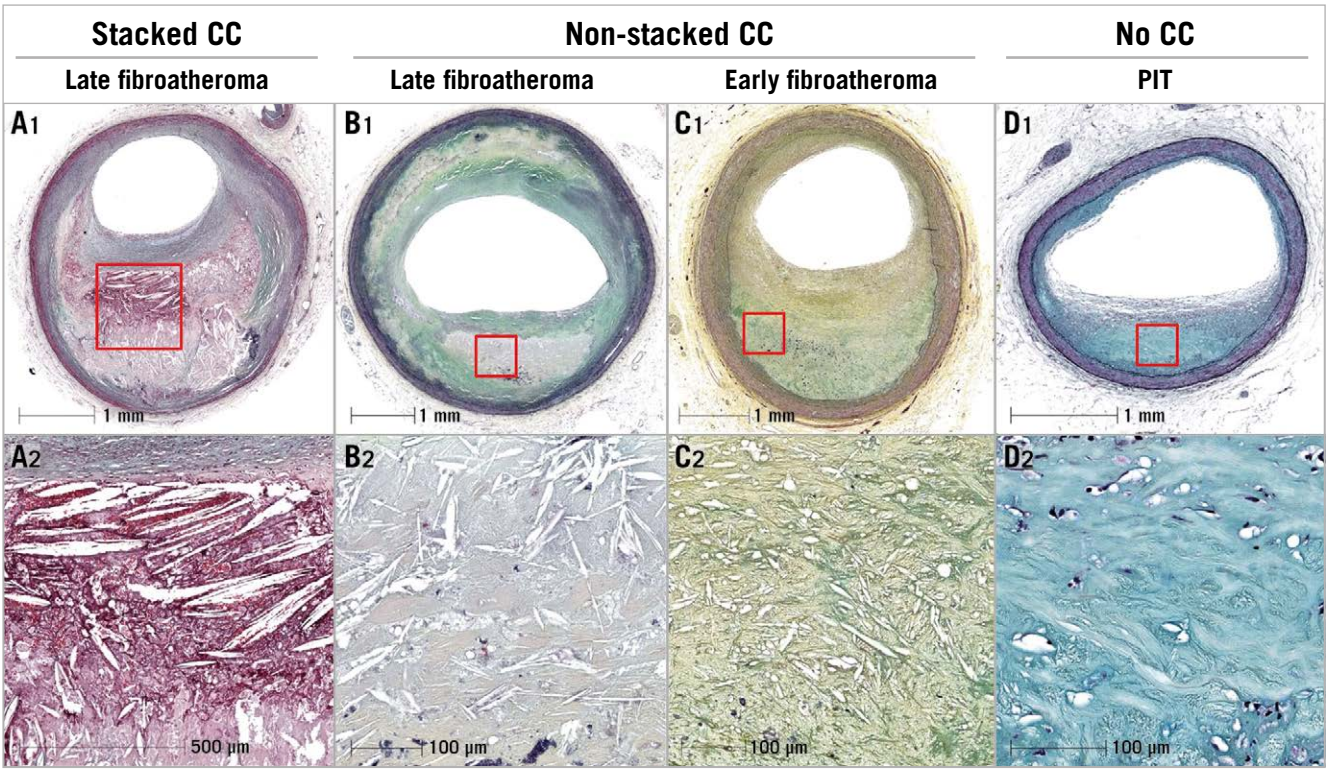

Figure 1. *Different types of cholesterol clefts (CC). A1) & A2) Low- and high-power images showing late necrotic core, stacked CC, haemorrhage, overlying fibrous tissue and severe luminal stenosis. B1) & B2) Low- and high-power images showing late fibroatheroma with small CC and moderate coronary stenosis. C1) & C2) Low- and high-power images showing early fibroatheroma, moderate luminal stenosis, thick fibrous cap and small CC. D1) & D2) Low- and high-power images showing pathological intimal thickening (PIT) lesion, lipid pool with absence of CC, and <50% luminal stenosis.*

plaque" has been broadly used by multiple investigators[4,5] but lacks specific detail. We defined CCR using the following criteria: 1) a linear, discrete, high-intensity signal (bright area) within the plaque; 2) a clear border must exist between this signal and adjacent low- or intermediate-intensity tissue; 3) the linear high-intensity signal is not a spot but a well-defined area distinguishing it from macrophages which lack sharp borders; and 4) it is not located at borders of calcification or within areas of calcification. When the diagnosis was inconsistent between the two readers, a consensus was achieved through discussion. Quantitative OFDI/OCT measurements were performed using a planimetry software (QIvus® 3.0; Medis medical imaging systems, Leiden, the Netherlands) **(Figure 2)**. Catheter-CCR angle was defined as the angle between the longitudinal line of the CCR and a line drawn from the centre of a catheter light sensor to the middle of the CCR. Depth of CCR was defined as the distance from the luminal surface to the middle of the CCR. Catheter-CCR distance was defined as the length from the centre of the catheter to the centre of the CCR.

STATISTICAL ANALYSIS

Details of the statistical analysis can be found in **Supplementary Appendix 1**.

Results

CLINICAL AND MORPHOLOGIC INFORMATION

Clinical characteristics of the vessels that had undergone OFDI or OCT are listed in **Table 1**. A total of 573 histologic cross-sections were available for histologic assessment and co-registration. Sections with processing artefact (n=4), post-mortem clot (n=4) and poor images (n=6) were not included in the analysis. A total of 559 images were co-registered with OFDI/OCT images for further analysis.

HISTOLOGIC ASSESSMENT OF THE TYPE OF PLAQUE AND PRESENCE OF CCR

Each histologic section (n=559) was classified by the type of plaque morphology: AIT/FIB 108 (19.3%), PIT 154 (27.5%), early FA 29 (5.2%), late FA 62 (11.1%), TCFA 15 (2.7%), plaque rupture 5 (0.9%), fibrocalcific (FC) + necrotic core 6 (1.1%), and FC 180 (32.2%) sections, respectively. A total of 117 sections showed presence of necrotic core **(Supplementary Table 1)** and all had histologic evidence of CC **(Figure 3)**. However, by OFDI/OCT, only 30 (25.6%) frames showed presence of CCR and all were also identified by histology with a positive predictive value (PPV) of 100.0%, negative predictive value (NPV) of 83.6%, with a sensitivity of 25.6%, specificity of 100.0% and accuracy of 84.4% **(Table 2, Table 3)**. Of 30 OFDI/OCT images

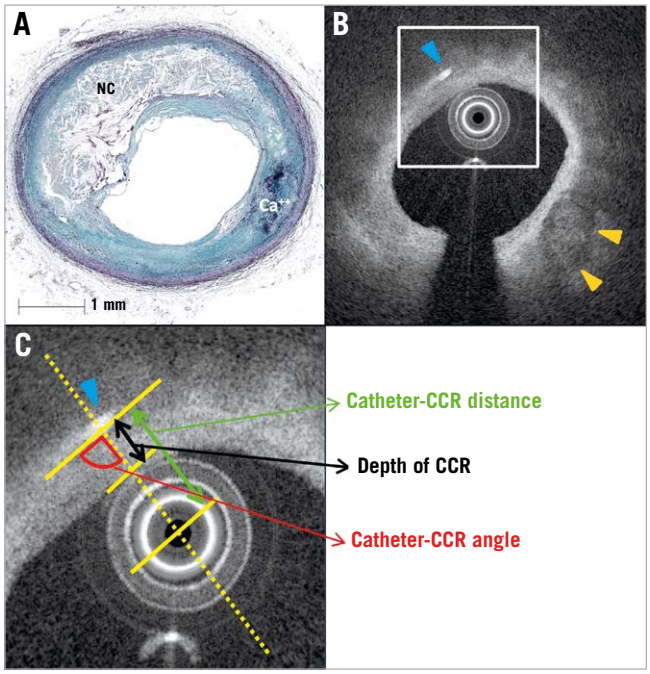

Figure 2. *Methods to evaluate OFDI/OCT-derived CCR. A) Histological image showing a fibroatheroma lesion with a necrotic core (Movat pentachrome stain). B) Co-registered OFDI cross-sectional image showing the presence of CCR (blue arrowhead) and calcification (orange arrowheads). C) High-power image of the white box from image B. Catheter-CCR distance is the distance between the centre of the sensor catheter tip and CCR (green double arrow); depth of CCR is the distance from the luminal surface of the catheter to the middle of CCR (black double arrow); and catheter-CCR angle is the angle between the longitudinal line of the CCR and the line from the centre of the catheter to the middle of CCR (red quarter-circle). Ca++: calcification; CCR: cholesterol crystals; NC: necrotic core; OCT: optical coherence tomography; OFDI: optical frequency domain imaging*

Table 1. Patient and vessel characteristics.

Patients		N=45
Age, years		56.3±13.6
Male		35 (77.8)
Past history	Hypertension	28 (62.2)
	Diabetes	9 (20.0)
	Hyperlipidaemia	7 (15.6)
	Smoker	13 (28.9)
Cause of death	SCD (acute)	11 (24.4)
	SCD (stable)	26 (57.8)
	Non-coronary artery death	2 (4.4)
	Non-cardiac death	6 (13.3)
Vessels		**N=55**
LAD		36 (65.5)
LCX		5 (9.1)
RCA		14 (25.5)

Values are mean±SD or n (%). LAD: left anterior descending coronary artery; LCX: left circumflex coronary artery; RCA: right coronary artery; SCD: sudden coronary death

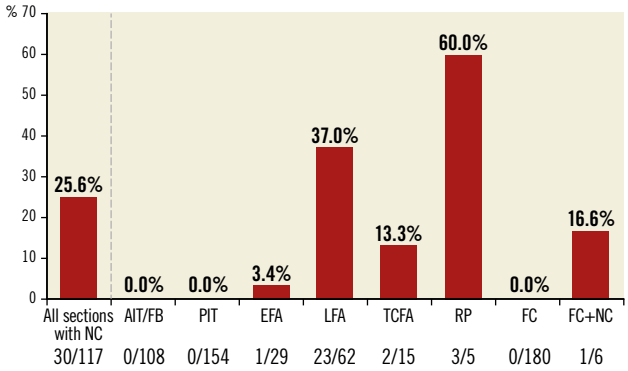

Figure 3. *Bar graph showing the distribution of CCR detectable by OFDI/OCT based on type of plaque. Plaque type was classified using histological images. Data are expressed as the total number of frames with CCR detected by OFDI/OCT over the total number of sections examined histologically stratified by plaque type. AIT: adaptive intimal thickening; CCR: cholesterol crystals; EFA: early fibroatheroma; FC: fibrocalcific plaque; FIB: fibrous plaque; LFA: late fibroatheroma; NC: necrotic core; OCT: optical coherence tomography; OFDI: optical frequency domain imaging; PIT: pathological intimal thickening; RP: plaque rupture; TCFA: thin-cap fibroatheroma*

Table 2. Detection of histological CC by OFDI/OCT.

OFDI/OCT	Histology		Total	Histology		Total
	CC+	CC–		Stacked CC+	Stacked CC–	
CCR+	30	0	30	26	4	30
CCR–	87	442	529	19	68	87
Total	117	442	559	45	72	117

CC: cholesterol clefts; CCR: cholesterol crystals; OCT: optical coherence tomography; OFDI: optical frequency domain imaging

showing CCR, the majority (86.7%) showed presence of stacked CC by histology. Stacked CC by histology were identified in 45 of 117 (38.5%) cases with necrotic core. The PPV, NPV, sensitivity, specificity and accuracy for detection of stacked CC by OCT/OFDI were 86.7%, 96.4%, 57.8%, 99.2% and 95.9%, respectively. **Figure 4** and **Supplementary Figure 1** show representative early and late FA, plaque haemorrhage, TCFA and rupture and corresponding OFDI/OCT images. **Supplementary Appendix 2** and **Supplementary Table 2** show aspects of the analysis.

COMPARISON OF DETECTABLE VERSUS UNDETECTABLE CCR BY OFDI/OCT TO THE MORPHOLOGIC FINDINGS

Of 117 sections with necrotic core by histology, 30 sections had detectable CCR and 87 sections no CCR by OFDI/OCT. Both groups underwent histologic measurements **(Table 4)**. In terms of basic morphometry (external elastic lamina [EEL], internal elastic lamina [IEL], lumen area and percent stenosis), there were no significant differences between the two groups. The tissue overlying (i.e., above) the CCR was assessed and showed significant

Table 3. PPV, NPV, sensitivity and specificity of OFDI/OCT for the detection of histological CC.

Type of CC in histology	PPV (95% CI)	NPV (95% CI)	Sensitivity (95% CI)	Specificity (95% CI)	Diagnostic accuracy (95% CI)
CC	100.0% (NA)	83.6% (82.0%-85.0%)	25.6% (18.0%-34.5%)	100.0% (99.2%-100.0%)	84.4% (81.2%-87.3%)
Stacked CC	86.7% (70.4%-94.7%)	96.4% (79.5%-97.4%)	57.8% (42.2%-72.3%)	99.2% (98.0%-99.8%)	95.9% (93.9%-97.4%)

CC: cholesterol clefts; CCR: cholesterol crystals; CI: confidence interval; NA: not applicable; NPV: negative predictive value; OCT: optical coherence tomography; OFDI: optical frequency domain imaging; PPV: positive predictive value

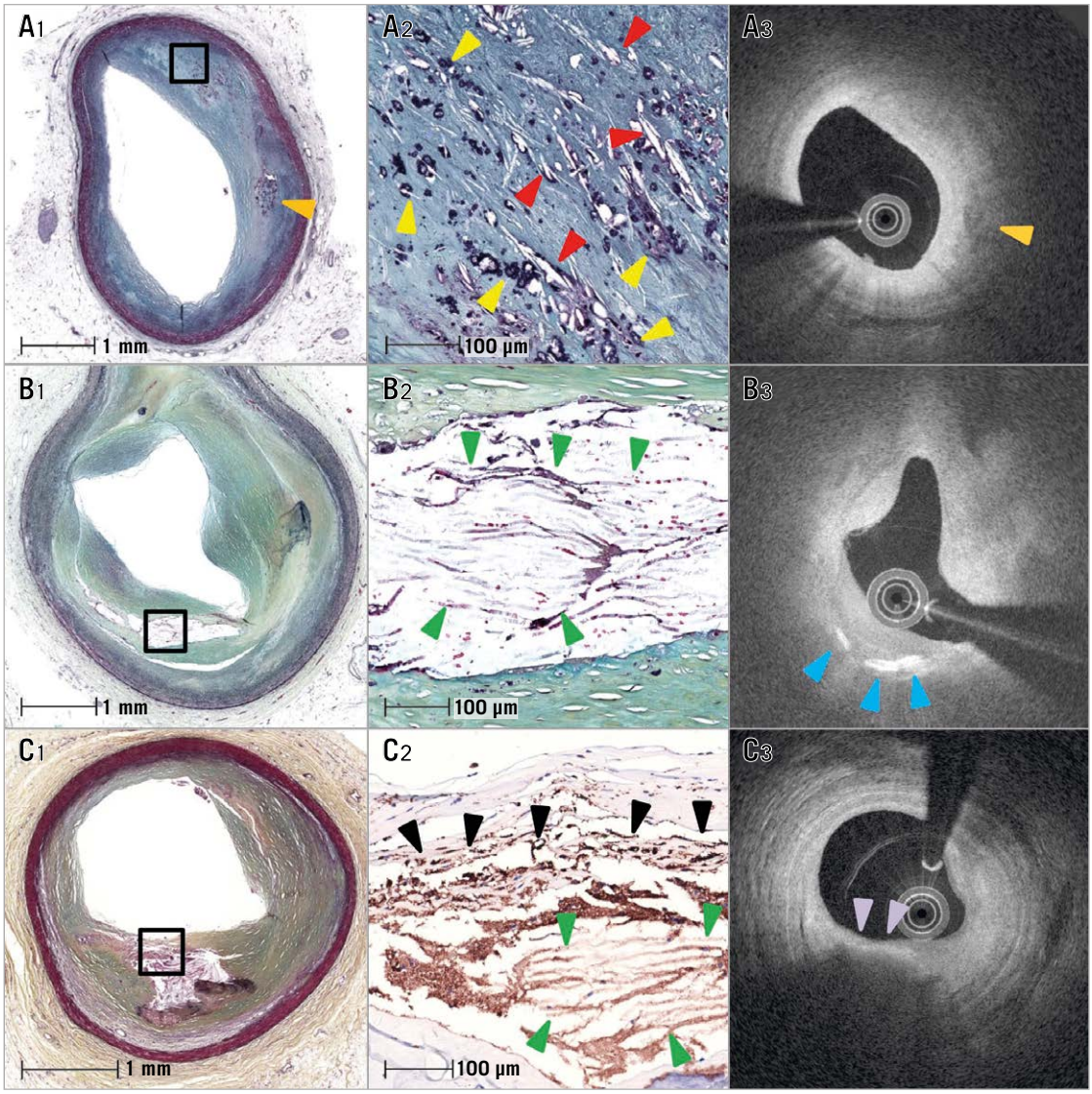

Figure 4. *Histological images of early and late fibroatheroma with corresponding OFDI images. A1) Low-power image showing early fibroatheroma with focal necrosis within the lipid pool, macrophage infiltration and calcification (orange arrowhead). A2) High-power image from A1 showing early necrotic core with interspersed CCR (red arrowheads) and punctate calcifications (yellow arrowheads) of macrophages. A3) OFDI image showing low-intensity area with absence of CCR and calcification (orange arrowhead) in the lipid pool. B1) & B2) Low- and corresponding high-power images of the boxed area showing a late fibroatheroma with a necrotic core area filled with stacked CC (green arrowheads). B3) OFDI image showing CCR (blue arrowheads). C1) & C2) Low- and high-power images showing a late fibroatheroma with stacked CC (green arrowheads) and overlying foamy macrophages (black arrowheads). High-power image (C2) is macrophage (CD68) stained image from the box in C1. C3) Corresponding OFDI image showing macrophages with attenuation (purple arrowheads) and no CCR. All histologic images are Movat stained except for C2 (CD68 staining). CC: cholesterol clefts; CCR: cholesterol crystals; OCT: optical coherence tomography; OFDI: optical frequency domain imaging*

Table 4. Histological measurements and characteristics.

Total number of sections (N=117)		Sections with detectable CCR by OFDI/OCT (n=30)	Sections without detectable CCR by OFDI/OCT (n=87)	*p*-value
Morphometric characteristics	EEL area, mm^2	15.3 (11.6-17.7)	15.5 (11.3-19.0)	0.60
	IEL area, mm^2	12.8 (10.5-15.6)	13.5 (9.5-16.5)	0.65
	Lumen area, mm^2	3.1 (2.5-3.9)	3.2 (2.0-4.5)	0.92
	Percent stenosis, %	74.4 (67.4-80.6)	73.9 (64.8-81.6)	0.69
	Thickness of fibrous cap, mm	0.33 (0.21-0.50)	0.44 (0.21-0.68)	0.042
	Area of necrotic core, mm^2	1.00 (0.39-2.21)	0.67 (0.28-1.60)	0.89
Stacked CC		26 (86.7)	19 (21.8)	<0.0001
Overlying tissue characteristics	Fibrous tissue	23 (76.7)	38 (43.7)	0.005
	PIT lesion	0 (0.0)	3 (3.5)	
	Foamy macrophages	4 (13.3)	37 (42.5)	
	Calcification	0 (0.0)	6 (6.9)	
	Thrombus	3 (10.0)	3 (3.5)	
Type of necrotic core	Early necrotic core	1 (3.3)	31 (35.6)	0.004
	Late necrotic core	29 (96.7)	56 (64.4)	
Presence of haemorrhage		17 (56.7)	21 (24.1)	0.002
Average length of CC, mm		0.25 (0.15-0.34)	0.11 (0.07-0.19)	<0.001
Average thickness of CC, µm		51.8 (17.8-76.3)	19.0 (10.7-30.3)	<0.0001

Values are median (interquartile range) or n (%). CC: cholesterol clefts; EEL: external elastic lamina; IEL: internal elastic lamina; PIT: pathological intimal thickening

differences between plaques with detectable and undetectable CCR, with more frequent fibrous tissue, and fewer foam cells and less thrombus in detectable CCR **(Figure 5A)**. Detectable CCR also showed a significantly higher prevalence of late necrotic core as compared to undetectable CCR. The presence of haemorrhage within the necrotic core was significantly more frequent in detectable CCR as compared to undetectable CCR. The length of the CC was also significantly greater in detectable versus non-detectable CCR. Detectable CCR showed significantly greater thickness of CC than undetectable.

OFDI/OCT MEASUREMENTS OF DETECTABLE CCR

In total, 42 CCR were observed in 30 frames. The depth of detectable CCR by OFDI/OCT was 0.43 mm (median, interquartile range [IQR]: 0.30-0.61 mm), and >95% of the CCR were less than 1.0 mm in depth. Catheter-CCR angle was 90.2° (median, IQR: 86.8-93.1°) and >95.0% CCR were seen at a catheter-CCR angle of 90±10° **(Table 5, Figure 5B)**.

MULTIVARIATE ANALYSIS FOR DETECTION OF CCR USING HISTOLOGICAL PARAMETERS

In univariate analysis, haemorrhage, stacked CC, late necrotic core, overlying fibrous tissue presence, CC length and thickness of fibrous cap showed significant differences between detectable and undetectable CCR by OFDI/OCT. Using these variables, multivariate analysis demonstrated that the presence of stacked CC and overlying fibrous tissue **(Table 6)** was highly predictive of OFDI/OCT identification of CCR.

Table 5. OFDI/OCT measurements of visible CCR.

	n=42
Distance from surface, mm	0.43 (0.30-0.61)
Distance from catheter, mm	1.34 (0.99-1.57)
CCR angle, °	90.20 (86.8-93.1)
Lipid arc, °	125.50 (82.8-168.8)
Length of CCR, mm	0.36 (0.27-0.52)
Thickness of CCR, mm	0.10 (0.07-0.14)

Values are median (interquartile range). CCR: cholesterol crystals; OCT: optical coherence tomography; OFDI: optical frequency domain imaging

Table 6. Multivariate analysis for detection of cholesterol crystals using histological parameters.

	Odds ratio	95% CI	*p*-value
Haemorrhage	1.21	0.34-4.30	0.77
Stacked CC	14.5	3.23-65.4	0.0001
Late necrotic core	4.56	0.42-50.0	0.17
Fibrous tissue as overlying tissue	6.02	1.74-20.8	0.003
CC length (increase 0.1 mm)	1.18	0.57-2.45	0.65
CC thickness (increase 1 µm)	0.99	0.96-1.01	0.31
Thickness of fibrous cap (increase 0.1 mm)	1.01	0.83-1.22	0.93

CC: cholesterol clefts; CI: confidence interval

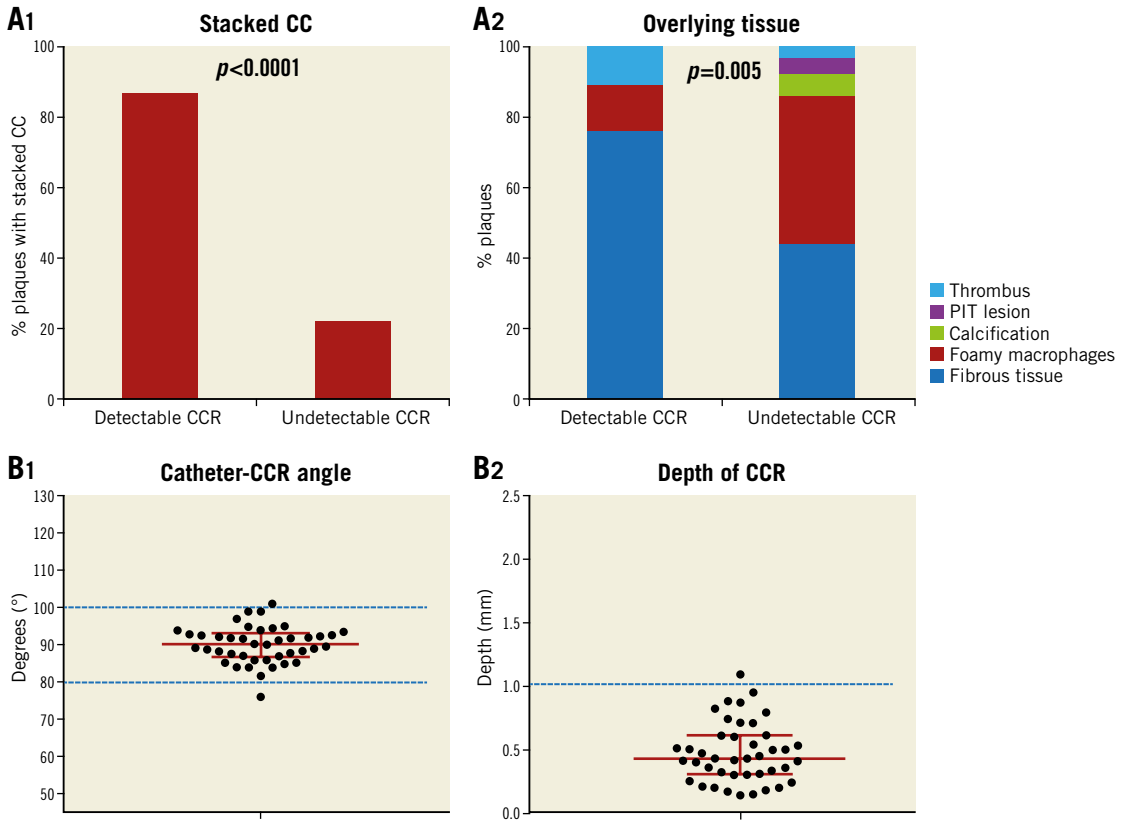

Figure 5. *Histological characteristics between detectable and undetectable CCR and OFDI/OCT findings of CCR. A1) Percent stacked CC in detectable and undetectable CCR by OFDI/OCT. A2) Overlying tissue characteristics in detectable and undetectable CCR by OFDI/OCT. B1) >95.0% CCR were seen at a catheter-CCR angle of 90±10°. B2) Depth of CCR from surface with majority located within 1 mm. Detectable CCR (n=30) and undetectable CCR (n=87). CC: cholesterol clefts; CCR: cholesterol crystals; OCT: optical coherence tomography; OFDI: optical frequency domain imaging; PIT: pathological intimal thickening*

Discussion

MAIN FINDINGS

This study is the first to examine the accuracy of OFDI/OCT for identification of the presence of CCR. In this study the primary findings were: 1) detection of CCR was low by OFDI/OCT; 2) advanced types of plaque (late FA, TCFA, and rupture) showed the presence of CCR by OFDI/OCT, whereas it was extremely rare within early FA; 3) a significant predictor for the detection of CCR by OFDI/OCT was the presence of overlying fibrous tissue and stacked CCR; 4) detectable CCR by OFDI/OCT were located within 1 mm from the luminal surface; and 5) longitudinal lines of the OFDI/OCT catheter sensor had to be close to 90° to the direction of CCR in order to visualise them.

Taken together, detectable CCR on OFDI/OCT mostly indicates the presence of stacked CC by histology and the presence of more advanced atherosclerotic lesions such as late necrotic core, presence of haemorrhage and large CC. Also, the detection of CCR was limited to advanced plaques; the presence of foamy macrophages or calcification above the CCR hindered the recognition of CCR by OFDI/OCT. Also, only CCR fulfilling specific optical conditions are detectable, i.e., angle and depth of OFDI/OCT are extremely important for the ability to recognise CCRs.

FREQUENCY OF OFDI- AND OCT-DERIVED CCR

As atherosclerosis progresses, plaque morphology changes based on stages of lesions. FA is the first clearly distinguishable plaque composed of lipid-rich necrotic core which consists of CC and cellular debris[1]. FA has been further subdivided histologically into early and late stages[1]. The former show presence of focal areas of necrotic core consisting of small CC and loss of proteoglycans and collagen in areas of macrophage infiltration, whereas the late FA show large areas of necrotic core composed of increasing numbers and larger size of CC, with complete lack of the extracellular matrix and collections of acellular debris[1]. TCFA and rupture also show presence of advanced necrotic core such as late FA; however, not all these lesions show OFDI/OCT-detectable CCR. Several clinical OCT/OFDI studies in living patients have detected the presence of CCR: these have varied from 17 to 24% in non-culprit sites[6,7]. CCR have been shown to be more frequent in acute coronary syndrome (ACS) patients and are recognised in 29-40% of culprit lesions requiring percutaneous coronary intervention for ACS or stable angina pectoris[4,5,8]. However, in clinical practice all types of lesion characteristics such as lipid pools, necrotic core, haemorrhage, and rupture are encountered. OFDI/OCT cannot distinguish between lipid pool

and necrotic core. Therefore, the presence of CCR by OFDI/OCT should be helpful to identify these CCR lesions as necrotic cores, which would help to distinguish them from PIT lesions which do not contain CCR.

Clinical presentations may also affect plaque components. A meta-analysis reported by Iannaccone et al showed that the prevalence of TCFA and rupture was higher in order of ST-elevation myocardial infarction (STEMI) >non-STEMI >unstable angina >stable angina[9]. Therefore, the manner of clinical presentation might also affect the prevalence of CC detection by OFDI/OCT. In our study, only 25.6% of sections with areas of necrotic core showed presence of CCR by OFDI/OCT. On the other hand, plaque rupture was present in five cases, three of which had CCR presence, thus indicating that the presence of CCR on OFDI/OCT may predict more advanced plaques that are likely to rupture. However, the rate of detection for CCR in TCFA was low; however, this may be due to the overlying tissue being rich in foamy macrophages, which hinders the identification of CCR by OFDI/OCT.

FACTORS TO DETECT OFDI/OCT-DERIVED CCR

Prior to our study, the significance of the presence of detectable CCR as detected by OFDI/OCT was unclear, although many OFDI and OCT studies included CCR as one of the atherosclerotic parameters assessed. This study showed factors that determine the visibility of CCR, i.e., presence of stacked CC and fibrous tissue overlying the CCR. Abela et al reported individual CCR measured by scanning electron microscopy and reported that the diameter of crystals varied from 1-3 µm at the tips and from 50 to 150 µm in length, and were up to 20 µm wide at the base[10]. This study also measured the longest length of CCR: the median was 250 µm (IQR 150 to 340 µm). However, because the resolution of OFDI/OCT is 10 to 20 µm, it is not surprising that most CCR cannot be identified as the width is <5 µm. We identified that stacked CC was the best predictor of the presence of CCR, probably due to their collective thickness exceeding 15 µm. Also, the type of tissue overlying CCR is important, with fibrous tissue allowing greater penetration while calcium and foamy macrophages hamper this penetration. This leads to the attenuation of the signals which results in the inability of OFDI/OCT to identify CCR. Late necrotic core typically shows increase in the numbers of single CCR in histological sections, and the presence of haemorrhage also contributes to the increase of CCR, as reported previously[11], which may allow OFDI/OCT to identify CCR.

CLINICAL IMPLICATION OF CCR

Intracoronary imaging devices do not possess the capability to distinguish lipid pools clearly in PIT lesions or the necrotic core in early FA from that in late FA. The presence of CCR indicates not simply necrotic core but more advanced necrotic core. The presence of OFDI/OCT-identified CCR from our study clearly shows that it reflects the presence of late FA. Our study shows that almost all detectable CCR are located in late necrotic core. Also, CCR correlated with the presence of plaque haemorrhage. Therefore, almost all lesions that show the presence of CCR by OFDI/OCT are advanced necrotic cores, and often show the presence of haemorrhage. In order to improve risk stratification and to guide therapy to prevent untoward cardiovascular events, the information from CCR may help us to understand the composition of advanced necrotic cores within plaques. Their presence by OFDI/OCT signifies an advanced lesion.

Limitations

First, all autopsy hearts were interrogated by intracoronary imaging devices in a blood-free environment, which is different from conditions in the catheterisation laboratory. However, all hearts were imaged during pressure perfusion with saline flush before formalin fixation; therefore, we believe that our findings remain valid and relevant to *in vivo* detection. Second, the study included non-cardiac and non-coronary death cases and a large majority of lesions were from stable sudden coronary death. Therefore, the incidence for the detection of CCR may be lower than if high-risk patients presenting with ACS had been included in the study.

Conclusions

OFDI/OCT is able to detect CCR within advanced atheromatous plaques although the sensitivity of OFDI/OCT for their detection was relatively low with higher specificity. The sensitivity was markedly improved by the presence of stacked CC with overlying tissue which attenuates the light signal. In addition to these two factors, optical conditions such as shallow depth and specific angle of CCR are important for the detection of CCR. The presence of CCR by OFDI/OCT suggests that the lesions are advanced.

Impact on daily practice

By histologic assessment at autopsy, detection for cholesterol crystals (CCR) by OFDI/OCT indicates stacked cholesterol clefts. The presence of CCR probably indicates advanced necrotic core (i.e., late necrotic core and plaque haemorrhage). This information from OFDI/OCT-detected CCR may help us to identify complicated atherosclerotic plaque in coronary arteries and improve risk stratification.

Funding

This study was funded by CVPath Institute, Inc., Gaithersburg, MD, USA.

Conflict of interest statement

R. Virmani has received institutional research support from Abbott Vascular, Boston Scientific and Terumo Corporation, honoraria from Abbott Vascular, Boston Scientific and Terumo Corporation, and is a consultant to Abbott Vascular, Boston Scientific and Terumo Corporation. A.V. Finn has received institutional research support from Abbott Vascular, Boston Scientific and Terumo

EuroIntervention 2020;16:395-403

Corporation, honoraria from Abbott Vascular, Boston Scientific and Terumo Corporation, and is a consultant to Abbott Vascular and Boston Scientific. The other authors have no conflicts of interest to declare.

References

1. Otsuka F, Joner M, Prati F, Virmani R, Narula J. Clinical classification of plaque morphology in coronary disease. *Nat Rev Cardiol.* 2014;11:379-89.

2. Duewell P, Kono H, Rayner KJ, Sirois CM, Vladimer G, Bauernfeind FG, Abela GS, Franchi L, Nunez G, Schnurr M, Espevik T, Lien E, Fitzgerald KA, Rock KL, Moore KJ, Wright SD, Hornung V, Latz E. NLRP3 inflammasomes are required for atherogenesis and activated by cholesterol crystals. *Nature.* 2010;464:1357-61.

3. Kotani J, Nanto S, Mintz GS, Kitakaze M, Ohara T, Morozumi T, Nagata S, Hori M. Plaque gruel of atheromatous coronary lesion may contribute to the no-reflow phenomenon in patients with acute coronary syndrome. *Circulation.* 2002;106:1672-7.

4. Dai J, Tian J, Hou J, Xing L, Liu S, Ma L, Yu H, Ren X, Dong N, Yu B. Association between cholesterol crystals and culprit lesion vulnerability in patients with acute coronary syndrome: An optical coherence tomography study. *Atherosclerosis.* 2016;247:111-7.

5. Fujiyoshi K, Minami Y, Ishida K, Kato A, Katsura A, Muramatsu Y, Sato T, Kakizaki R, Nemoto T, Hashimoto T, Sato N, Meguro K, Shimohama T, Tojo T, Ako J. Incidence, factors, and clinical significance of cholesterol crystals in coronary plaque: An optical coherence tomography study. *Atherosclerosis.* 2019;283:79-84.

6. Hou J, Xing L, Jia H, Vergallo R, Soeda T, Minami Y, Hu S, Yang S, Zhang S, Lee H, Yu B, Jang IK. Comparison of Intensive Versus Moderate Lipid-Lowering Therapy on Fibrous Cap and Atheroma Volume of Coronary Lipid-Rich Plaque Using Serial Optical Coherence Tomography and Intravascular Ultrasound Imaging. *Am J Cardiol.* 2016;117:800-6.

7. Xing L, Higuma T, Wang Z, Aguirre AD, Mizuno K, Takano M, Dauerman HL, Park SJ, Jang Y, Kim CJ, Kim SJ, Choi SY, Itoh T, Uemura S, Lowe H, Walters DL, Barlis P, Lee S, Lerman A, Toma C, Tan JWC, Yamamoto E, Bryniarski K, Dai J, Zanchin T, Zhang S, Yu B, Lee H, Fujimoto J, Fuster V, Jang IK. Clinical Significance of Lipid-Rich Plaque Detected by Optical Coherence Tomography: A 4-Year Follow-Up Study. *J Am Coll Cardiol.* 2017;69:2502-13.

8. Kataoka Y, Puri R, Hammadah M, Duggal B, Uno K, Kapadia SR, Tuzcu EM, Nissen SE, King P, Nicholls SJ. Sex Differences in Nonculprit Coronary Plaque Microstructures on Frequency-Domain Optical Coherence Tomography in Acute Coronary Syndromes and Stable Coronary Artery Disease. *Circ Cardiovasc Imaging.* 2016 Aug;9(8).

9. Iannaccone M, Quadri G, Taha S, D'Ascenzo F, Montefusco A, Omede P, Jang IK, Niccoli G, Souteyrand G, Yundai C, Toutouzas K, Benedetto S, Barbero U, Annone U, Lonni E, Imori Y, Biondi-Zoccai G, Templin C, Moretti C, Luscher TF, Gaita F. Prevalence and predictors of culprit plaque rupture at OCT in patients with coronary artery disease: a meta-analysis. *Eur Heart J Cardiovasc Imaging.* 2016;17:1128-37.

10. Abela GS, Aziz K, Vedre A, Pathak DR, Talbott JD, Dejong J. Effect of cholesterol crystals on plaques and intima in arteries of patients with acute coronary and cerebrovascular syndromes. *Am J Cardiol.* 2009;103:959-68.

11. Virmani R, Burke AP, Farb A, Kolodgie FD. Pathology of the vulnerable plaque. *J Am Coll Cardiol.* 2006;47:C13-8.

Supplementary data

Supplementary Appendix 1. Methods.

Supplementary Appendix 2. Results.

Supplementary Figure 1. Histological images of intraplaque haemorrhage, thin-cap fibroatheroma and rupture with corresponding OFDI/OCT images.

Supplementary Table 1. Assessment of plaque morphologies by OFDI and OCT.

Supplementary Table 2. Assessment of the commonly used definition for cholesterol crystals as "high linear signal within the plaque".

The supplementary data are published online at: https://eurointervention.pcronline.com/doi/10.4244/EIJ-D-20-00202

Supplementary data

Supplementary Appendix 1. Methods

Study population

Autopsy hearts received from the medical examiner that had consecutively undergone OFDI or OCT were available from the CVPath autopsy registry during the period from September 2016 to February 2019.

OFDI/OCT imaging procedure

Following gross and radiographic examination of the hearts, the left main and right coronary arteries were cannulated and angiography was performed. If any of the four major coronary arteries showed greater than 30% diameter stenosis, these were further imaged using either OFDI (Terumo Corporation, Tokyo, Japan) or OCT (Abbott Vascular, Santa Clara, CA, USA) catheters. In order to maintain physiological vessel dimensions, all procedures were performed before pressure fixation with 10% neutral buffered formalin. OFDI/OCT was not attempted in cases with occlusive thrombus. An imaging catheter was advanced over a 0.014-inch guidewire, previously deployed under fluoroscopy. For improvement of imaging quality, vessels were continually flushed with phosphate buffered at low pressure by a non-pulsatile pump. Each imaging run was performed at a pullback speed of 10 or 20 mm/s (frame rate 160 frames/s) by OFDI or OCT. The data obtained were transferred to an offline station for co-registration.

Histology processing for coronary arteries

The coronary arteries were cut at 3-4 mm intervals and embedded in paraffin. The coronary arteries were removed from the heart, radiographed and decalcified when required, and cut into 2 to 3 cm segments with the proximal segments inked and dehydrated. Each paraffin block was sectioned at 4-6 μm and four sections cut with the first two sections stained with haematoxylin and eosin and modified Movat pentachrome stains.

Morphometrical analysis in histology

Histological morphometry was performed using ZEN 2 (blue edition) (Carl Zeiss, Oberkochen, Germany) to assess the area of the external elastic lamina (EEL), internal elastic lamina (IEL), lumen area, necrotic core area, thickness of fibrous cap (the thinnest part of the fibrous cap) and length of CC defined as the average length of the three largest CC.

Statistical analysis

Continuous variables were expressed as mean±standard deviation or median and interquartile range (IQR) depending on distribution of data after normality of distribution was confirmed by the Shapiro-Wilk test. Confidence intervals for positive predictive value (PPV), negative predictive value (NPV), sensitivity, specificity and accuracy are “exact” Clopper-Pearson confidence intervals. For section-level analysis the generalised estimating equation (GEE)

method was used. Categorical data were tested by the GEE method with an ordinal logistic model or tubular Fisher's exact test, as appropriate. In multivariate analysis for detection of CCR by OFDI/OCT, variables that showed a p-value of <0.1 in univariate analysis were used. For evaluation of inter- and intra-observer variation in interpretation, CCR and types of plaque in OFDI/OCT were recorded blindly by the observers and analysed by Cohen's kappa statistic. A p-value of <0.05 was considered statistically significant. JMP software, version 13.0 (SAS, Cary, NC, USA) and SPSS software, Version 19 (IBM Corp., Armonk, NY, USA) were used for statistical analyses.

Supplementary Appendix 2. Results

Histologic assessment of the types of plaque and presence of CCR

The overall intra-observer κ coefficient for diagnosing tissue type and CCR was 0.75 and 0.80, respectively, and the overall inter-observer κ coefficient was 0.76 and 0.79, respectively.

Using the standard definition of CCR as "high linear signal within the plaque" similarly to previous investigators, 108 of 559 sections showed high linear signal within the plaque. Of these 108 sections, CC were observed on microscopy in 30 (27.8%), 26 (24.1%) were within areas of calcification, 23 (21.3%) had foamy macrophages, 24 (22.2%) occurred at the borders of calcification, and 5 (4.6%) occurred in an area of smooth muscle cells in a proteoglycan matrix (the κ-values for intra- and inter-observer variability were 0.74 and 0.70, respectively). Therefore, if this definition was applied without further modification, there would be a large number of false positive cases **(Supplementary Table 2)**.

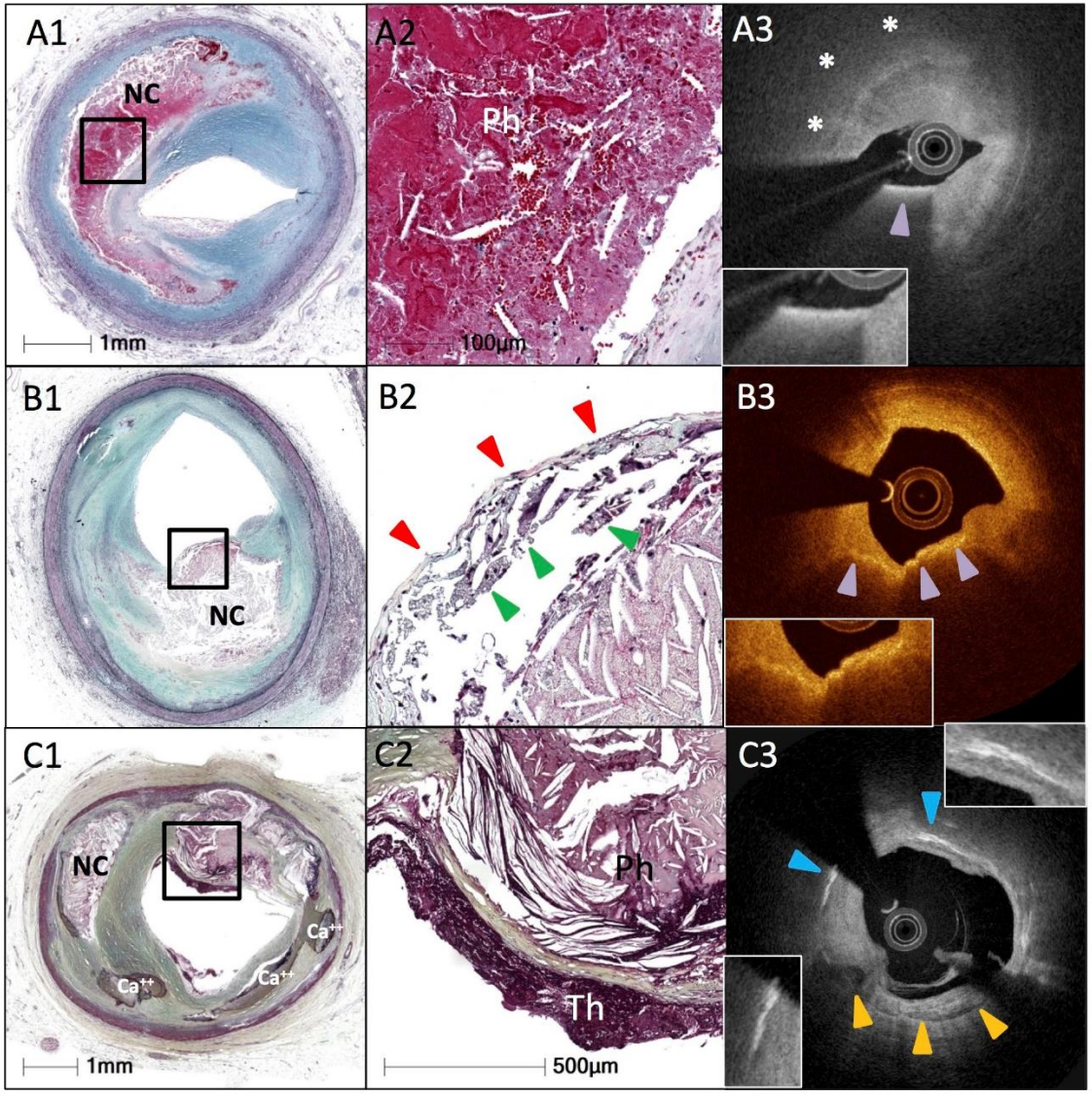
A1
NC
1mm
A2
Ph
100µm
A3
B1
NC
B2
B3
C1
NC
Ca++
Ca++
Ca++
1mm
C2
Ph
Th
500µm
C3

Supplementary Figure 1. Histological images of intraplaque haemorrhage, thin-cap fibroatheroma and rupture with corresponding OFDI/OCT images.

A1) & A2) Low- and high-power images showing a large necrotic core with acute plaque haemorrhage consisting of red blood cells and fibrin but few, small CC and absence of stacked CC.

A3) OFDI image showing low-intensity signal indicating lipid pool (white asterisk) and macrophages (purple arrowhead) but no CCR can be identified.

B1) & B2) Low- and high-power images showing thin-cap fibroatheroma with foamy macrophages (green arrowheads) infiltrating the thin cap (red arrowheads) and underlying necrotic core with individual CC but no stacking.

B3) Corresponding OCT shows presence of OCT macrophages (purple arrowheads) but no CCR can be identified.

C1) & C2) Low- and high-power images showing plaque rupture with stacked CC in the necrotic core, plaque haemorrhage and superficial thrombus.

C3) Corresponding OFDI image showing CCR (blue arrows) in lipid pool and calcifications (orange arrowheads). All histologic images are Movat stained.

Ca++: calcification; CC: cholesterol clefts; CCR: cholesterol crystals; NC: necrotic core, OCT: optical coherence tomography; OFDI: optical frequency domain imaging; Ph: plaque haemorrhage; Th: thrombus

Supplementary Table 1. Assessment of plaque morphologies by OFDI and OCT.

	OFDI/OCT					
	Fibrous	Lipid rich	TCFA	Rupture	Fibrocalcific	Total
Histology						
AIT/fibrous	94	14	0	0	0	108
Pathological intimal thickening	32	120	1	0	1	154
Early fibroatheroma	0	24	0	0	5	**29**
Late fibroatheroma	0	51	1	0	10	**62**
TCFA	0	5	9	0	1	**15**
Rupture	0	1	0	4	0	**5**
Fibrocalcific+necrotic core	0	2	1	0	3	**6**
Fibrocalcific	0	10	0	0	170	180
Total	126	227	12	4	190	559

Histological diagnoses with necrotic core are **bold** (a total of 117 sections).
AIT: adaptive intimal thickening; OCT: optical coherence tomography; OFDI: optical frequency domain imaging; PIT: pathological intimal thickening; TCFA: thin-cap fibroatheroma

Supplementary Table 2. Assessment of the commonly used definition for cholesterol crystals as "high linear signal within the plaque".

	N=108
Cholesterol crystals	30 (27.8%)
Foamy macrophages	23 (21.3%)
Inside of calcification	26 (24.1%)
Border of calcification	24 (22.2%)
An area of smooth muscle cells in a proteoglycan matrix	5 (4.6%)

Values are expressed as number of sections (%).